Mon. Not. R. Astron. Soc. **000**, 000–000 (0000) Printed 22 February 2000 (MN LaTeX style file v1.4)

Simultaneous optical polarimetry and X-ray data of the near synchronous polar RX J2115–5840

Gavin Ramsay[1], Stephen Potter[1,2], Mark Cropper[1], David A. H. Buckley[2], M. K. Harrop-Allin[1]

[1] *Mullard Space Science Laboratory, University College London, Holmbury St.Mary, Dorking, Surrey, RH5 6NT*
[2] *South African Astronomical Observatory, PO Box 9, Observatory 7935, Cape Town, South Africa*

22 February 2000

ABSTRACT

We present simultaneous optical polarimetry and X-ray data of the near synchronous polar RX J2115–5840. We model the polarisation data using the Stokes imaging technique of Potter et al. We find that the data are best modelled using a relatively high binary inclination and a small angle between the magnetic and spin axes. We find that for all spin-orbit beat phases, a significant proportion of the accretion flow is directed onto the lower hemisphere of the white dwarf, producing negative circular polarisation. Only for a small fraction of the beat cycle is a proportion of the flow directed onto the upper hemisphere. However, the accretion flow never occurs near the upper magnetic pole, whatever the orientation of the magnetic poles. This indicates the presence of a non-dipole field with the field strength at the upper pole significantly higher. We find that the brightest parts of the hard X-ray emitting region and the cyclotron region are closely coincident.

Key words: binaries: individual: RX J2115–5840, EUVE 2115–58.6, stars: magnetic fields - stars: variables

1 INTRODUCTION

Polars (or AM Her systems) are amongst the most suitable objects with which to study the interaction between an accretion flow and a magnetic field. This is because the magnetic field of the accreting white dwarf is strong enough (B ∼10–200MG) to prevent the formation of an accretion disk. Therefore, the dominating emission source at all wavelengths is the post-shock region above the surface of the white dwarf. In polars, the spin period of the white dwarf and the binary orbital period are generally synchronised and the accretion flow from the dwarf secondary star threads onto magnetic fields lines which have an unchanging orientation with respect to the white dwarf (see Cropper 1990 and Beuermann & Burwitz 1995 for general reviews of polars).

However, four systems are known to be slightly (∼ 1%) asynchronous (the near synchronous polars) and the accretion flow will therefore attach onto different field lines as the flow rotates around the white dwarf on the timescale of the spin-orbit beat period. Until very recently, observations covering a beat period have been difficult to obtain because the beat period is weeks or more (V1432 Aql: Watson et al 1995, Friedrich et al 1996, Geckeler & Staubert 1997; BY Cam: Silber et al 1997, Mason et al 1998) or the system is faint (V1500 Cyg: Stockman, Schmidt & Lamb 1988). Now a fourth system (RX J2115–58) which is reasonably bright (V ∼17) has been discovered with a beat period of 6.3 days (Schwope et al 1997, Ramsay et al 1999) which allows a detailed study of these systems to be undertaken for the first time.

The observations of Ramsay et al (1999) made over 13 nights in 1997 provide the most direct evidence that the accretion flow is directed onto one magnetic pole and then the other as the flow rotates around the white dwarf on the timescale of the beat period. This is most apparent in the circular polarisation data which shows a change of sign when the accreting flow is directed onto opposite magnetic poles. From these observations they determined the spin period of the white dwarf to be P_{ω}=109.55 mins and the binary orbital period to be P_{Ω}=110.89 mins.

The observations of Ramsay et al (1999) were difficult to reconcile with simple views of how the accretion stream attaches onto the magnetic field of the white dwarf. To investigate this in greater detail we have obtained simultaneous optical polarisation and X-ray data obtained using *RXTE* in July 1998.

Date	Telescope	HJD Start	Duration
Optical Polarimetry			
1998 July 21	SAAO 1.9m	16.37	7h 20m
1998 July 22	SAAO 1.9m	17.36	6h 25m
1998 July 23	SAAO 1.9m	18.34	5h 30m
1998 July 24	SAAO 1.9m	19.31	7h 25m
1998 July 25	SAAO 1.9m	20.32	8h 20m
1998 July 26	SAAO 1.9m	21.31	8h 35m
X-ray			
1998 July 21	*RXTE*	16.59	7.6ksec
1998 July 22	*RXTE*	17.59	7.9ksec
1998 July 23	*RXTE*	18.53	13.2ksec
1998 July 24	*RXTE*	19.55	6.9ksec
1998 July 25	*RXTE*	20.53	13.1ksec
1998 July 26	*RXTE*	21.57	6.9ksec
1998 July 27	*RXTE*	22.50	14.2ksec

Table 1. Observing log for RX J2115–580. The HJD the start time is HJD+2451000.0.

2 OBSERVATIONS

2.1 Polarimetry Data

White light optical polarimetry data were obtained using the SAAO 1.9m telescope at Sutherland, South Africa and the UCT Polarimeter (Cropper 1985). Table 1 details these observations. There were occasions when thin cloud was present which compromised some of the photometry but did not effect the polarisation data. The data were reduced as described in Cropper (1997).

Ramsay et al (1999) made the point that the circular polarisation data is the most useful aspect of the polarisation data because the sign change of the circular polarisation data indicates a change in accreting pole. Taking this lead we initially concentrate on the circular polarisation data.

As in the 1997 data, our new data have some nights which show positive and negative polarisation and also other nights when only one sign of polarisation was seen (Fig. 1). However, in contrast to the 1997 data, which were reasonably repeatable over the course of one night, the new data are more variable. For instance, the peak in negative circular polarisation seen at HJD=2451016.4 is not repeated during the night. More interestingly, a negative circular polarisation peak is expected at HJD=2451021.42 based on the timing of the peaks that night; however, none is seen. Checks (such as determining how the sky polarisation varied over the course of the night) were made to determine if this could be due to instrumental problems, but we have ruled these out. The lack of a polarisation peak therefore implies that the accretion flow is being directed equally towards both poles and the net polarisation is zero, or that the accretion flow is very unstable and can 'switch-off' on timescales as short as one orbital period. The fact that there is no dip in the intensity curve at this point suggests that the former scenario is more likely.

A Discrete Fourier Transform (DFT) was used to search for periodic signals in the data. The amplitude spectrum is similar to that of the 1997 data (Fig. 2 of Ramsay et al 1999) although the resolution is lower since only 6 nights are covered. The amplitude spectrum was pre-whitened using the spin and orbital frequencies (and their first harmonics and $P_\omega \pm P_\Omega$ side bands) detected in the 1997 data and shown in Table 1 of Ramsay et al (1999). There were no remaining frequencies with an amplitude above 0.1 percent and we find no evidence for any other side band frequencies. To examine how the polarisation data varies over the spin-orbit beat period, we show in Figure 2 these data folded on the spin period as a function of the beat period. Since we do not know the beat period accurately enough to phase our new data with that of our 1997 data, we have matched the beat phase of our new data so that it approximately matches that of the 1997 data (to within ~0.1 cycles). The phasing of the spin phase is arbitrary. We discuss these data in detail in §4.

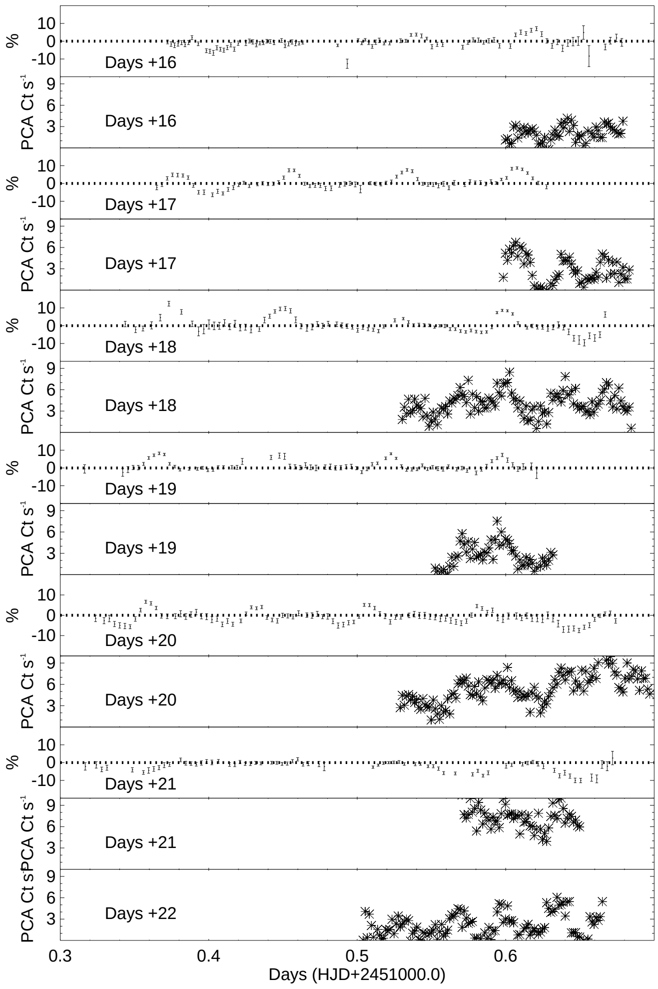

Figure 1. The circular polarisation data and *RXTE* PCA (2–15keV) data. The HJD is shown on the left hand side +2451000.0.

2.2 X-ray data

RX J2115–58 was detected in the 2-15 keV range using *RXTE* when it was observed in 1998 July 21–27 (Table 1). To improve the signal-to-noise ratio, we extracted data from only the top Xenon layer of the PCA. The background was estimated using `PCABACKEST` V2.1b using the faint source

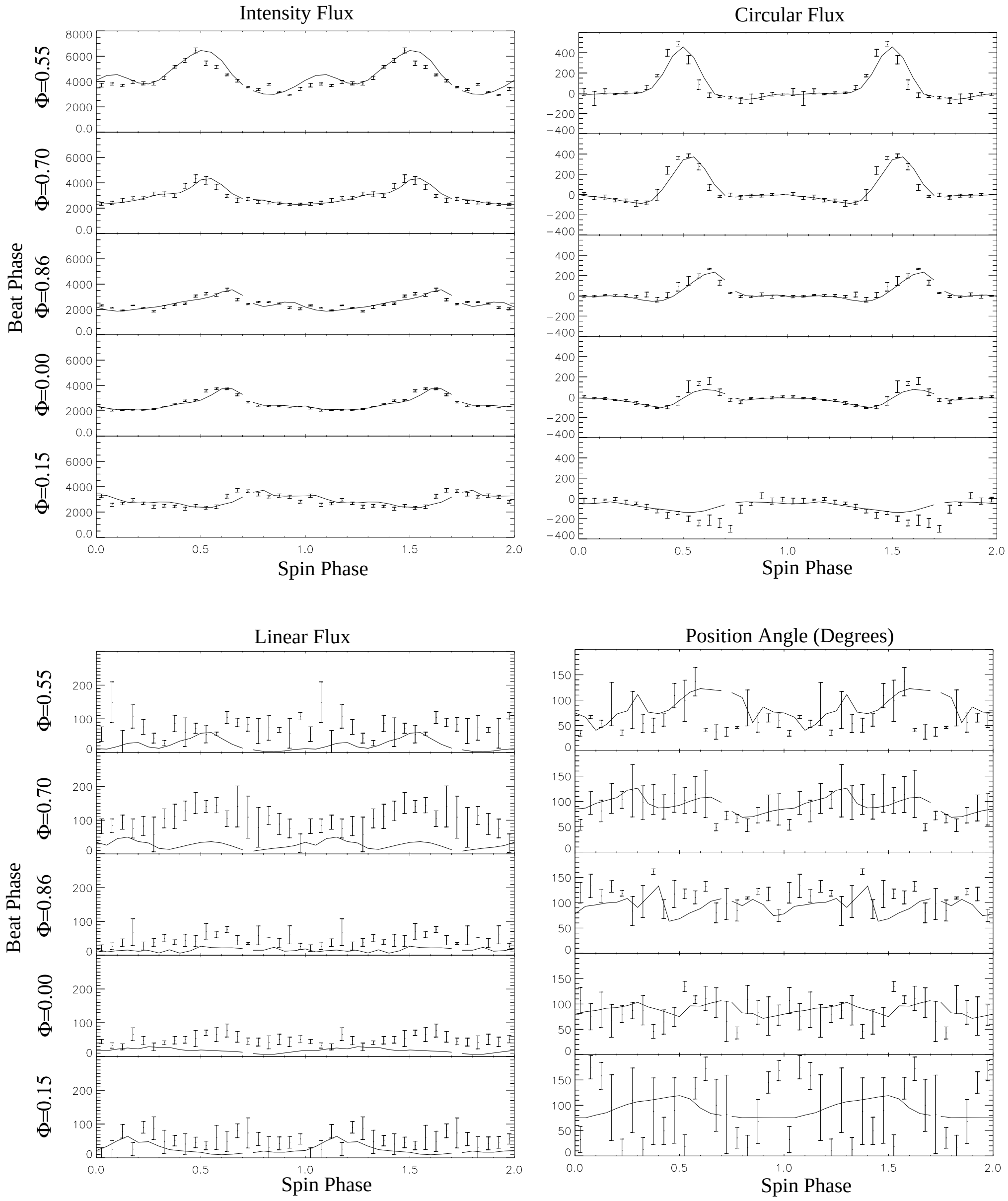

Figure 2. The polarisation and intensity data folded on the spin period together with the model fits for various spin-orbit beat phases. Phase zero of the beat phase has been chosen so that it matches approximately that of beat phase of Ramsay et al (1999). The phasing of the spin period is arbitrary.

models applicable to the date of the observation. After excluding data contaminated by high background rates, we were left with 65 ksec of data with a mean background subtracted count rate of 3.9 ct s^{-1}.

The background subtracted light curve using the full 2-15 keV range is also shown in Fig. 1. Unlike many polars the amplitude of the variation is comparatively small. There are, however, bright peaks in the light curve which correspond to peaks in the white light intensity curve and the peaks in the circular polarisation curve.

As for the circular polarisation data we used a DFT to search for periodic modulations in the X-ray light curve. A peak is found which corresponds to the spin frequency. Its amplitude is much less prominent compared to the amplitude spectrum of the circular polarisation data. The data were pre-whitened using the spin and orbital frequencies (and their first harmonics and $P_\omega \pm P_\Omega$ side bands) as for the optical data: no additional significant peaks were found.

To examine the intensity variation as a function of the beat period, we show in Fig 3 the X-ray data folded on the spin period as a function of the beat period. The shape of the spin-folded light curve varies quite considerably during the beat cycle. The modulation is rather low at beat phase ψ=0.35 and 0.72. On the other hand a large peak is seen in the spin-folded data at beat phase ψ=0.56. We searched for any hardness variation in the spin-folded light curves by dividing the 2–4keV folded and binned data with the equivalent 4–15keV data for all beat phases: no evidence was found for a significant variation. We go onto discuss the X-ray spectrum of RX J2115–58 in more detail in §5 and

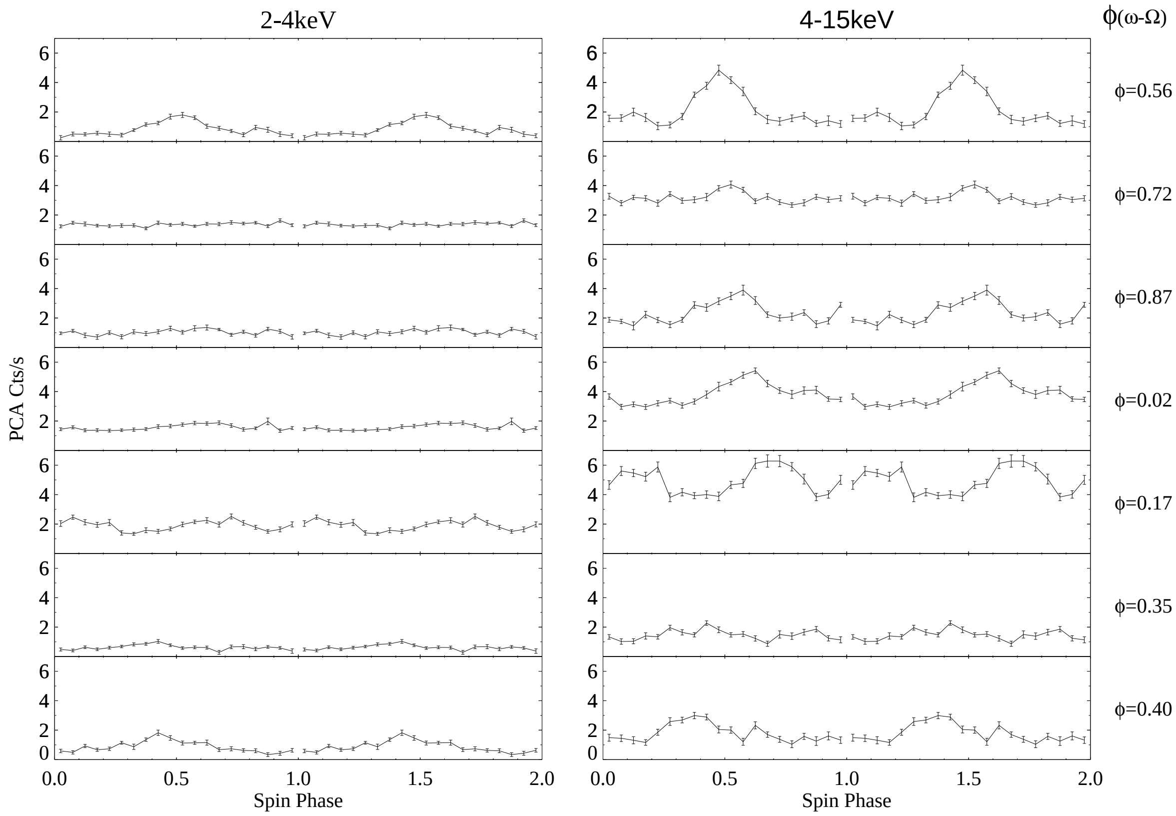

Figure 3. The X-ray data folded on the spin period as a function of the spin-orbit beat period for two energy bands. These data have been phased in the same manner as our optical data.

possible explanations for the change in the spin-folded light curves in §6.

3 THE SPIN AND ORBITAL PERIODS OF RX J2115–58

Determining accurate orbital and spin periods of near synchronous polars is far from trivial. This is because if the accretion flow is directed onto one then the other pole during the spin-orbital beat cycle – a 'pole-switch' – different periods can be obtained for observations covering different fractions of the beat cycle (Mouchet et al 1997).

The most comprehensive set of observations of RX J2115–58 is that of the polarimetry data of Ramsay et al (1999) which covered a time interval of 13 days. They determined a spin period, P_{ω}=109.55 mins and an orbital period of P_{Ω}=110.89 mins. This orbital period is very similar to that determined by Vennes et al (1996) (110.8 mins) who obtained 4 nights of spectroscopy over a time span of 6 days. Another slightly longer orbital period (111.3 mins) was determined by Buxton et al (1999) who obtained spectroscopic data on 5 consecutive nights. To further complicate matters, Schlegel (1999) analysed *ROSAT* HRI data and tentatively found 2 periods, 102.6 and 110.4 mins which did not coincide with any other period determinations.

We do not place great weight to the periods determined by Schlegel (1999) since they were determined from data lasting only 14.8 ksec (just over 2 spin cycles) which was spread over 59 ksec. On the other hand, the period determined by Buxton et al (1999) deserves further comment. In an analysis of the near synchronous polar BY Cam (with a beat period of 14.5 days), Mouchet et al (1997) found that the period determinations in that system were biased depending on the time interval over which they were collected. It is likely that this can account for the difference between the orbital period determinations of Buxton et al (1999), Vennes et al (1996) and Ramsay et al (1999). Since the polarisation data of Ramsay et al (1999) covers the longest time interval (~1.4 beat cycles), it is probable that these period determinations have the least bias.

Although the amplitude spectra of the X-ray and polarimetric data presented in this paper are consistent with the periods determined by Ramsay et al (1999), we must regard these periods with some degree of caution until they can be confirmed. Nevertheless, to make progress, we assume these periods for the rest of this paper. Unfortunately, these periods are not precise enough to phase together the data in Ramsay et al (1999) and the data presented here.

4 MODELLING THE POLARIMETRY DATA

4.1 Background

To model our polarisation data we used the optimisation method (Stokes imaging) of Potter, Hakala & Cropper (1998). This method finds the best fit to the data and maps the shape, location and structure of the cyclotron emission region(s) in an objective manner. Stokes imaging finds the smoothest solution using a regularisation technique. It has been successfully used to fit data on other polars, eg MN

Hya (Ramsay & Wheatley 1998), V347 Pav (Potter et al 2000) and ST LMi (Potter 2000).

Strictly speaking, the model maps the accretion region(s) in terms of an optical depth parameter. In this paper we assume a simple dipole field and the cyclotron model at the core of the Stokes imaging is a 10 keV constant temperature model of Wickramasinghe & Meggitt (1985) which is suitable for modelling white light observations (Potter 2000). We used a dipole magnetic field strength of 15 MG. This is consistent with that found by Vennes et al 1996 ($\lesssim$20 MG) and Schwope et al 1997 (11$\pm$2 MG). In fact, the resulting fits to white light data are not affected by small changes to the magnetic field strength (Potter 2000).

The aim of the Stokes Imaging technique is to produce highly resolved images of the emission regions as they change from one beat phase to the next. However, in the case of our data, the time resolution of the data is only 20 points per spin phase of the white dwarf. Therefore one data point corresponds to 18 degrees of rotation by the white dwarf. Thus the maximum resolution of the map would be 18 square degrees. In practice, it is slightly worse than this because of the regularisation term which smooths the images, and also because the amount of polarised flux, especially the linear flux, is not particularly high. This will therefore result in blurred images of the cyclotron emission regions. However, the main aim here is to investigate how the emission regions move across the surface of the white dwarf from one beat phase to the next. Thus, even though the image resolution is quite low, any systematic movement of the region across the surface of the white dwarf will be evident in the cyclotron emission maps.

4.2 Preliminary fits to the data

As the system is near synchronous we need to construct a different accretion map for each beat phase. Figure 1 shows that even during the course of a single night the accretion geometry can change. To obtain accurate maps of the accretion region(s) we need good phase resolution and small errors on the folded and binned data points. We therefore have chosen time intervals in which the polarisation data was repeatable. Naturally, in those intervals when the data was not repeatable, this would lead to significant changes in the resulting accretion maps. For instance at HJD=2451021.42 (§2.1 and Figure 1) where a negative circular polarisation peak was not seen when expected, the accretion map would be very different at that epoch. We return to this point in §6.

Since this system is not eclipsing and there has been no detailed modelling of polarisation data until now to give us an indication of the system geometry, we initially had to search a wide range of parameter space. The binary inclination, i, was searched between i =0–80°, the angle between the binary inclination and the magnetic axis, β, was searched between β=0–90°, and the phase at which magnetic pole crosses our line of sight, ζ, was searched between ζ=0–360°.

For all the beat phase intervals that we observed, we found the best fit solutions had high inclinations, low dipole offsets and the phase at which the magnetic pole crosses our line of sight ζ corresponds to spin phase 0.25. Outside this parameter range the fits were very poor. Although i and β are not strongly constrained we can rule out low inclinations and high dipole offsets. The data are not of sufficient quality to allow us to constrain the angles further.

In our fitting routine all four Stokes parameters are equally weighted. However, because the sign of the circular polarisation is an indicator of which magnetic hemisphere of the white dwarf accretion is occurring, we consider the fit to the circular polarisation data to be the most important parameter when it comes to examining the fits by eye. In addition, unlike the intensity data (which will be contaminated by other non-accretion driven sources) it is pure cyclotron emission. Upon inspection of the final fitness values of all the solutions (a parameter which indicates the goodness of fit and the smoothness of the map, Potter, Hakala & Cropper 1998), we find that the fits to the circular polarisation are significantly better for inclinations above 60° and dipole offsets less than 20°. In the next stage of our modelling we kept these parameters fixed at the following values for each beat phase: $i = 70°$, $\beta = 10°$, $\zeta = 90°$. These values are not necessarily the best values for a particular beat phase, but they are however the best values that give good fits for all beat phases.

4.3 Detailed fits to the data

The model polarisation curves along with the data are shown in Fig. 2. The fits to the intensity data are good, as are the fits to the circular polarisation with the exception of the beat phase ψ=0.15. On the other hand the linear polarisation data is consistently underestimated in our model. This is a result of two effects. Firstly the lower count rate in the linear flux and hence the relatively larger error bars compared to the intensity and circular flux will result in the linear flux not having a large effect in the fitting procedure. Secondly, the large size of the emission regions that have arisen due to the low time resolution of the data will lead to the smoothing of any linearly polarised features. The emission maps are shown in a Mercator projection in Fig. 4 for 5 spin-orbit beat phases. We also show the emission regions projected onto a globe as a function of spin phase for two spin-orbit beat phases in Fig. 5 & 6.

The maps shown in Fig. 4 show how the location of the emission regions change over the beat cycle. The location of the magnetic poles and the equator are also shown. Emission regions on opposite magnetic hemispheres will, of course, exhibit circular polarisation of opposite sign when viewed at the same orientation. For the majority of the beat period which we were able to observe, significant emission is present only in the lower hemisphere. Only at beat phase ψ=0.15 is there significant emission present in the upper hemisphere – this is the only beat phase where there is a negative peak in circular polarisation (Fig. 2). All other beat phases have positive circular polarisation peaks. We therefore conclude that cyclotron emission from the lower hemisphere is positively circularly polarised while in the upper hemisphere it is negatively polarised.

Because of the orientation of the binary system, the accretion region in the lower hemisphere appears at the edge of the visible disk of the white dwarf (Fig. 5 & 6). At beat phase ψ=0.15 this region is visible for only a very short proportion of the spin cycle and the majority of the accretion is directed onto the upper hemisphere. Caution should be exercised when interpreting the structure of the accretion region in the upper hemisphere (Fig. 6) since the fit to the circular polarisation data is rather poor between spin phases $\phi \sim$0.5–0.8 when this accretion region is in view. All we can say with confidence is that accretion is taking place onto the upper hemisphere at these spin phases rather than the lower hemisphere. We discuss the results of these polarisation maps, together with the X-ray light curves, in more detail in §6. However, we now go onto discuss the X-ray light curves with these accretion maps in mind.

5 MODELLING THE X-RAY DATA

It is reasonable to assume that the polarised optical flux and the hard X-ray flux originate from the same shock region above the white dwarf. It should be possible, therefore, to use the cyclotron opacity maps derived in the previous section as an indication of the hard X-ray emission region. We have therefore constructed a simple model that uses the cyclotron maps to produce the hard X-ray emission one would expect from such an region, assuming optically thin X-ray emission. This is only possible because we have quasi-simultaneous optical and X-ray data. However, for beat phases ψ=0.35 and ψ=0.40 this is not possible since we do not have the cyclotron opacity maps for these beat phases. We also assume that the map of the optical depth parameter is an indication of the density of the X-ray emitting region and, hence, higher densities give more hard X-ray flux.

In Figure 7 we show model hard X-ray light curves overlaid on top of the hard X-ray data. The model light curves have been normalised to the data. We stress that the model light curves are a prediction of the hard X-ray flux and have not been fitted to the data. Good fits are, therefore, not expected but where there are major differences between data and model we can arrive at some tentative conclusions.

Firstly, the general agreement between the model and the data is rather good. In particular, the maximum peak in the model X-ray light curves agrees very well with the shift in the observed peak from one beat phase to the next. This suggests that brightest X-ray and polarised emission regions are indeed closely coincident. A closer inspection of beat phase ψ = 0.56 shows that the model has over-estimated the amount of X-ray flux at spin phases ϕ=0.1–0.4. This can either imply that the X-rays are being absorbed, perhaps by the accretion stream, or the X-ray emitting region is somewhat less extended than the cyclotron emission region. Examining Figure 5, it is not clear that the orientation of the stream is such that the X-rays from the accretion region would be heavily absorbed at spin phases ϕ=0.1–0.4. On the other hand, the actual extension of the cyclotron emission region is difficult to determine accurately at the moment due to the low time resolution of the polarimetric data. Similarly for beat phases ψ = 0.02 and ψ = 0.17 there is excess model X-ray flux at certain spin phases.

We now go on to examine the X-ray spectrum of RX J2115–5840. A mean background subtracted PCA X-ray spectrum covering 21–27 July 1998 was extracted over the 2-15keV energy range and binned to improve the signal to noise. The spectrum was fitted with a range of models con-

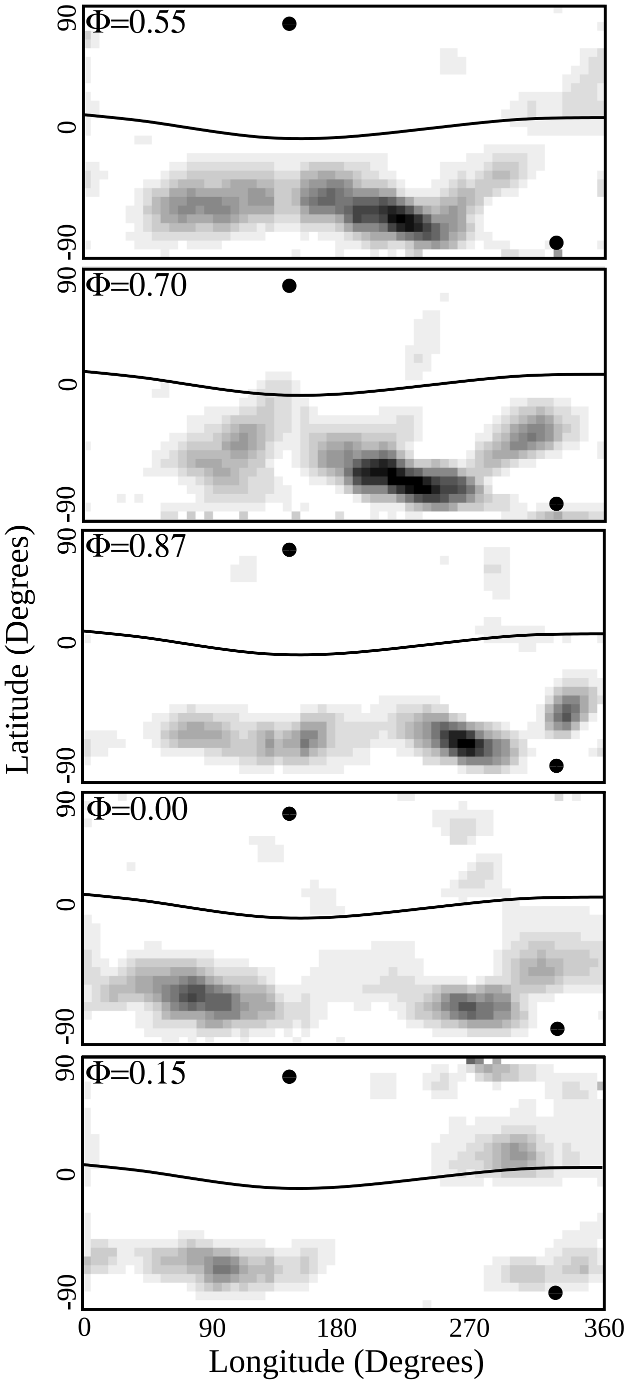

Figure 4. The accretion regions on the white dwarf are shown in spin coordinates as a function of beat phase. The dark dots mark the locations of the magnetic poles and the magnetic equator is shown as a solid line. The upper magnetic pole points most favourably to the observer at spin phase ϕ=0.25 (§4.2).

sisting of variations of an absorbed hot thermal plasma (eg a cold absorber plus thermal bremsstrahlung, a cold absorber and partially ionised absorber plus a hot thermal plasma, cf Cropper, Ramsay & Wu 1998). A good fit could not be achieved – the best fit gave a χ^2_ν=2.12 (31 dof). The largest source of error between the models and the data were at energies less than 4keV. At these energies, absorption effects

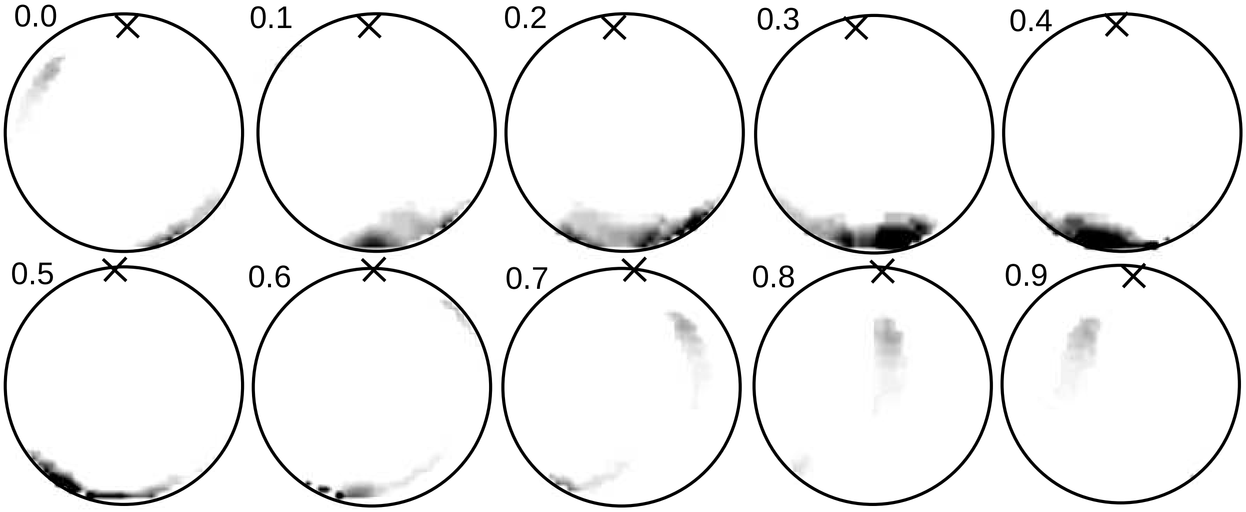

Figure 5. The location of the accretion regions for the spin-orbit beat phase ψ=0.55 as predicted by our model. The spin phase of the white dwarf is shown while the cross marks the location of the upper magnetic pole.

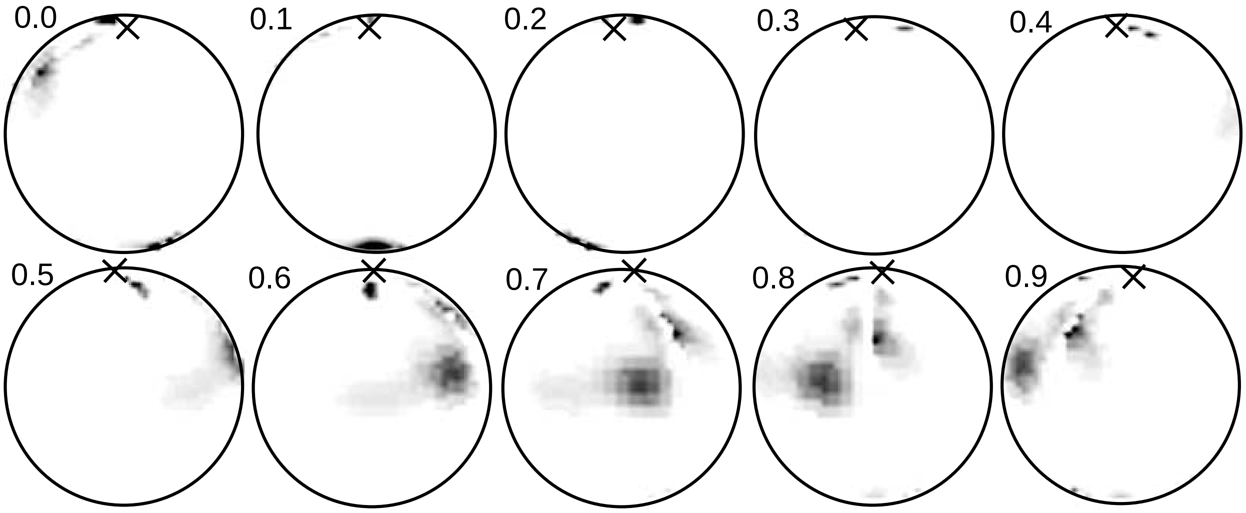

Figure 6. As Figure 5 but for the spin-orbit beat phase ψ=0.15.

at the base of the post-shock flow, where it merges with the white dwarf, become important and are difficult to model. This is consistent with the results discussed above which suggest that at certain beat and spin phases, the effects of absorption is evident.

To make some progress in extracting information from our X-ray spectrum, we excluded data softer than 4keV. At energies harder than this the absorbing column can be modelled using a simple cold absorber rather than a more complex one such as a partial covering model. While the data could be adequately modelled using an absorbed optically thin plasma, (such as the `MEKAL` model), we chose to use a multi-temperature model (Wu, Chanmugam & Shaviv 1994) as implemented by Cropper, Ramsay & Wu (1998) and improved to take into account the effects of gravity over the height of the post-shock flow (Cropper et al 1999). This model allows us to determine parameters such as mass of the white dwarf and the local mass accretion rate. Our model also takes into account the fact that some fraction of the accretion luminosity is radiated in optical/IR wavelengths through cyclotron radiation. The relative proportion of the cyclotron component increases with increasing magnetic field strength.

Using the above multi-temperature model and a cold absorber a good fit to the data was achieved (χ^2_ν=1.16: 23 degrees of freedom). In this model, the ratio of cyclotron to thermal bremsstrahlung cooling, ϵ_o, was fixed at 1.0 at the shock: this gave an inferred magnetic field strength at the accretion region of $B \sim$15 MG. Since the accretion regions are offset from their respective magnetic poles, we do not expect the field at the accretion regions to match the dipole field strength. However the resulting fit is not very sensitive to this parameter and almost unchanged solutions result from field strengths between 10–20 MG. Our chosen value matches that used for our polarimetry model fits. The viewing angle was fixed at 30° although this parameter has a very small effect on the resulting white dwarf mass (varying this parameter between 0–90° changes the mass by 0.01 $M_\odot$). Figure 8 shows the fit to the data using this model while Table 2 shows the best fit parameters.

Ramsay et al (1999) suggested that their polarimetry data implied the accretion regions had different magnetic

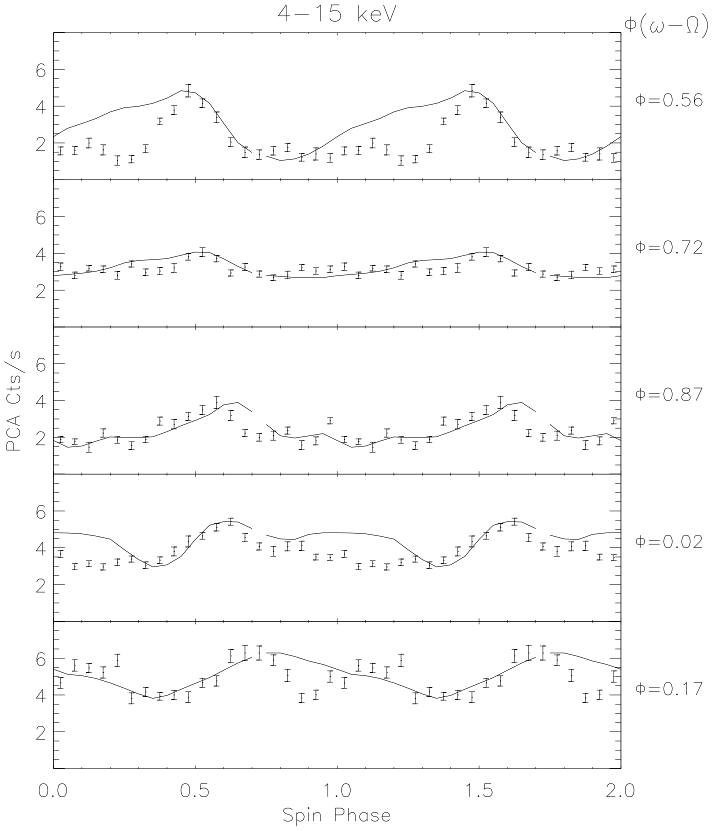

Figure 7. The X-ray data (4–15keV) overlaid with the model X-ray light curve obtained using the maps of the location and extent of the emission regions derived using the polarisation mapping. The close agreement between the phasing of the peaks of the data and model suggest a close coincidence between the brightest part of the hard X-ray and cyclotron emitting regions.

N_H	7.3×10^{20} cm^{-2}
$\dot{m}$	0.99 g s^{-1} cm^{-2}
Z	0.53 solar
M_1	0.79 (0.68–0.91) $M_\odot$
χ^2_ν	1.16 (23 dof)
Observed flux	8.5×10^{-12} erg s^{-1} cm^{-2}
Unabsorbed flux	9.9×10^{-12} erg s^{-1} cm^{-2}

Table 2. The best fits to the mean background subtracted PCA spectrum (4–15keV). The model is an absorbed multi-temperature thermal bremsstrahlung model. Z is the metal abundance relative to solar, M_1, is the mass of the white dwarf and the values in brackets refer to the 90 per cent confidence range. The two flux measurements are the implied flux over the 4–15keV energy range.

field strengths, indicating evidence for a dipole offset or a magnetic field geometry more complex than a simple dipole. This is consistent with the observation of Schwope et al (1997) who found that at one epoch RX J2115 was bright in the EUV and at another epoch much stronger in hard X-rays. If there was a large dipole offset then it is expected that there would be a significant difference in the hard X-ray spectra of the two accreting poles.

We extracted the X-ray data originating from each pole by assuming that at epochs when only positive circular was

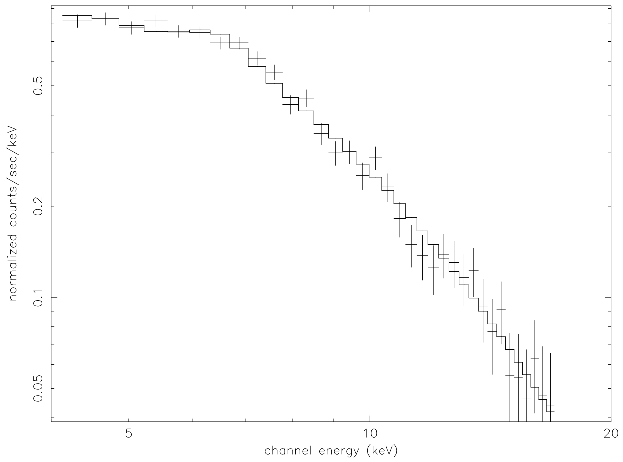

Figure 8. The fit to the mean background subtracted *RXTE* PCA X-ray spectrum. The model is an absorbed multi-temperature model – see text for details.

detected accretion was occurring on to only one pole. When only negative polarisation was detected accretion was occurring onto the other pole. These two spectra were fitted using the same best fit model to the mean spectrum with only the normalisation being allowed to vary. Good fits (χ^2_ν<1.05) were obtained to both spectra indicating that there is no evidence (from these data) for a significant difference in the hard X-ray spectra from each accreting pole. The data from each night were also fitted with the best fit model and equally good fits were found. We conclude that these X-ray data are consistent with a simple dipole magnetic field as used for the polarisation modelling.

6 THE MOVING ACCRETION REGIONS IN RX J2115–58

Ramsay et al (1999) presented polarisation data covering a large fraction of the spin-orbit beat interval. Using these data they proposed a very preliminary model in which the accretion flow was directed onto one or other footprint of the same magnetic field line at all beat phases. The main accretion regions on opposite hemispheres were fixed to within $\sim 70^\circ$ in magnetic longitude. With the detailed modelling of our new data presented here, it is possible to test the preliminary model of Ramsay et al (1999).

We first concentrate on the accretion pattern in the lower hemisphere, in which accretion occurs at all beat phases where we have been able to Stokes Image the data. Figure 4 shows that at beat phase ψ ~0.55 an extended accretion region is seen in this hemisphere. As we increase in beat phase, we find that the brightest (strictly speaking the most dense) part of the accretion region advances in positive longitude: between beat phase ψ=0.55 and 0.85, we find it has increased in spin longitude by $\sim 50^\circ$ from $\sim 220-270^\circ$. This shift is also seen in the advancement in spin phase of the peak of the positive circular polarisation in Fig. 2 (also seen in Ramsay et al 1999), and is consistent with our X-ray data. During this interval the region also splits into two distinct components separated by $\sim 180^\circ$ in longitude – this has clearly occurred by beat phase ψ=0.00. Slightly later, at beat phase $\psi = 0.15$, for a short phase interval, the originally most prominent region in the lower hemisphere is almost absent, and accretion occurs onto the upper hemisphere. This new region is located near the longitude of the lower magnetic pole. At this beat phase, the two accretion regions are therefore approximately 180° in longitude from their respective magnetic poles. Alternatively, they are at the expected longitudes, but at the opposite latitudes to that expected. We are unable to account for this behaviour at this beat phase. However, it is clear that accretion never occurs near the upper pole, whatever the azimuth of the magnetic poles. This probably indicates the presence of a non-dipole field with the field strength at the upper pole significantly higher, in agreement with the suggestion of Schwope et al (1997) and despite the lack of evidence from our X-ray data.

Ramsay et al (1999) suggested that at beat phase $\psi = 0.00$ it is possible that the stream divides close to the white dwarf so that one stream accretes most directly and the other follows a path around the white dwarf. Alternatively, and in our view more likely, the stream separates much closer to the secondary star and follows a path some distance in azimuth around the white dwarf before accreting. As we move further in beat phase (to ψ=0.15), we find the accretion region which was located at 270° in longitude (Figure 4) has become much reduced and the accretion flow onto the lower hemisphere is directed onto the accretion spot at 90° in longitude. It is also at this point in the beat cycle that accretion is directed onto the upper hemisphere. By the time of our next accretion map (ψ=0.55), we find that the first accretion footprint is again the most favourable and this is where the bulk of the accretion flow is directed.

We return finally to the cycle-to-cycle variability of the circular polarisation evident in Figure 1. This appears to be most marked at the beat phases at which the circular polarisation is predominantly negative, ie those beat phases around $\psi = 0.15$ when the accretion occurs in the upper hemisphere. The variability is therefore most likely caused by changes in the balance of the accretion flow to upper and lower hemispheres via the two streams, resulting in a net polarisation of approximately zero.

7 ACKNOWLEDGMENTS

We would to thank the Director of SAAO, Dr R Stobie, for the generous allocation of observing time and we are grateful to Dr D O'Donoghue for the use of his period analysis software.

REFERENCES

Beuermann, K., Burwitz, V., 1995, In 'Cape Workshop on mCVs', eds Buckley, D. A. H., Warner, B., ASP Conf Ser, Vol 85, p99
Buxton, M., Vennes, S., Wickramasinghe, D. T., Ferrario, L., 1999, In 'Annapolis workshop on magnetic CVs', ASP Conf Series, Vol 157, p.223
Cropper, M., 1985, MNRAS, 212, 709
Cropper, M., 1990, Space Sci Rev, 54, 195
Cropper, M., 1997, MNRAS, 289, 21
Cropper, M., Ramsay, G., Wu, K., 1998, MNRAS, 293, 222
Cropper, M., Wu, K., Ramsay, G., Kocabiyik, A., 1999, MNRAS, 306, 684
Friedrich, S. et al 1996, A&A, 306, 860
Geckeler, R. D., Staubert, R., 1997, A&A, 325, 1070
Mason, P. A., Ramsay, G., Andronov, I., Kolesnikov, S., Shakhovskoy, N. & Pavlenko, E., 1998, MNRAS, 295, 511
Mouchet, M., Bonnet-Bidaud, J. M., Somov, N. N., Somova, T. A., 1997, A&A, 324, 109
Potter, S. B., 2000, in press, MNRAS
Potter, S. B., Hakala, P., Cropper, M., 1998, MNRAS, 297, 1261
Potter, S. B., Cropper, M., Hakala, P., 2000, submitted, MNRAS
Ramsay, G., Wheatley, P. J., 1998, MNRAS, 301, 95
Ramsay, G., Buckley, D. A. H., Cropper, M., Harrop-Allin, M. K., 1999, MNRAS, 303, 96
Schlegel, E. M., 1999, AJ, 117, 2494
Schwope, A. D., Buckley, D. A. H., O'Donoghue, D., Hasinger, G., Trümper, J., Voges, W., 1997, AA, 326, 195
Silber, A., et al 1997, MNRAS, 290, 25
Stockman, H. S., Schmidt, G. D., Lamb, D. Q., 1988, ApJ, 332, 282
Vennes, S., Wickramasinghe, D. T., Thorstensen, J. R., Christian, D. J., Bessell, M. S., 1996, AJ, 112, 2254
Watson, M. G., et al 1995, MNRAS, 273, 681
Wickramasinghe, D. T., Meggitt, S. M. A., 1985, MNRAS, 214, 605
Wu, K., Chanmugam, G., Shaviv, G., 1994, ApJ, 426, 664